J. Am. Chem. Soc. **1980**, *102*, 5151-5157

Proton Affinities and Photoelectron Spectra of Three-Membered-Ring Heterocycles

Donald H. Aue,*[1a] Hugh M. Webb,[1a] William R. Davidson,[1a] Mariano Vidal,[1a] Michael T. Bowers,[1a] Harold Goldwhite,[1b] Lawrence E. Vertal,[1b] John E. Douglas,[1c] Peter A. Kollman,[1c] and George L. Kenyon[1c]

Contribution from the Department of Chemistry, University of California, Santa Barbara, Santa Barbara, California 93106, the Department of Chemistry, California State University, Los Angeles, Los Angeles, California 90032, and the Department of Pharmaceutical Chemistry, School of Pharmacy, University of California, San Francisco, San Francisco, California 94143. *Received October 22, 1979*

Abstract: Proton affinities and photoelectron spectra have been measured for azirane, phosphirane, oxirane, and thiirane and for the corresponding dimethylamine, phosphine, ether, and sulfide. The photoelectron spectra have been fully assigned by the use of ab initio STO-431G calculations and structural correlations within these series of molecules. The lone-pair ionization potentials of the heterocycles are higher than those of their open-chain dimethyl analogues because of charge redistribution effects in the C–X bonds and increased lone-pair s character in azirane and phosphirane. The proton affinities are lower in the heterocycles than in their dimethyl analogues as a result of increases in lone-pair s character and, especially for phosphirane, an increase in the RXR angle strain on protonation. Ab initio calculations on the protonated heterocycles and XH_n models are presented to help interpret the proton-affinity data.

Introduction

Bond-angle changes about a central atom can strongly alter the electronic properties of a molecule. Exploration of these effects helps to define the nature of chemical bonding in such molecules. Three-membered heterocycles provide examples of molecules in which these bond-angle changes are carried to an extreme relative to unconstrained heteroatomic systems of normal bond angles. We concentrate our attention here on a simple set of three-membered heterocycles containing nitrogen, phosphorus, oxygen, and sulfur, viz., azirane, phosphirane, oxirane, and thiirane. The gas-phase basicities and photoelectron spectra of these molecules have been measured and compared with those of dimethylamine, dimethylphosphine, dimethyl ether, and dimethyl sulfide, respectively. Guided by these results and by molecular-orbital calculations, we seek to understand the consequences of bond-angle changes and hybridization effects on the lone-pair basicities and ionization potentials of these heterocycles. From our previous work on azirane and oxirane, it appears that their proton affinities correlate with lone-pair hybridization changes.[2a] Phosphirane and thiirane have been studied to determine whether such effects operate in heterocycles containing third-row elements.

Experimental Section

Samples of azirane and thiirane were obtained from Aldrich Chemical Co. and distilled before use. Oxirane was obtained from Matheson Gas Products. Phosphirane was prepared according to a published procedure.[2b]

Gas-phase basicities were measured by trapped ion cell and drift cell ion cyclotron resonance techniques previously described.[3,4] Photoelectron spectra were obtained on a Perkin-Elmer PS-18 photoelectron spectrometer with a resolution of ca. 30–40 mV at 12 eV. The vertical IPs were measured at the maxima of the band intensities, and the adiabatic IPs were measured at the onset of the first band.[3] Spectra were calibrated with an internal xenon and argon standard, with an estimated accuracy of ±0.03 eV for vIPs and ±0.1 eV for aIPs.

The ab initio calculations were carried out using the program GAUSSIAN 70[5] with STO-3G[6] and STO-431G[7] basic sets.

Results and Discussion

Photoelectron Spectra. The photoelectron spectra for the three-membered N, P, O, and S heterocycles and their corresponding dimethyl derivatives are summarized in Tables I and II. The photoelectron spectra for phosphirane and thiirane are reported for the first time and are reproduced in Figures 1 and 2. Our spectra for azirane and oxirane agree well with those reported earlier.[8] The photoelectron spectrum for azirane has been assigned on the basis of double-ζ level calculations by Basch and co-workers.[8] The first three orbitals are of a′, a″, and a′ symmetries. The highest energy orbital (n) is pictured below, while the next two orbitals have the character of the antisymmetric (σ_a) and symmetric (σ_s) Walsh orbitals of cyclopropane.[8-10] Double-ζ level calculations on oxirane (see Table I) show the first two orbitals (a_1 and b_1) to be nearly accidentally degenerate, but calculation of the first two IPs by correction for electronic reorganization and correlation energies indicates that the b_1 orbital, with lone-pair character, is higher in energy.[8] This appears clearly to be true experimentally, since the vibrational Franck–Condon factors for the first band are typical of oxygen lone-pair orbitals in ethers.[11] The next two bands are Walsh-type orbitals, but they show the opposite order from those in azirane with the a_1 (σ_s) orbital at higher energy than the b_2 (σ_a) orbital.

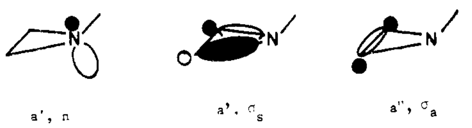

The photoelectron spectra for phosphirane and thiirane have been assigned from the 4-31G (double-ζ) calculations summarized in Table I. Experimentally determined geometries were used in all such calculations in Tables I and II. These calculations agree reasonably well with experiment and lead to a clear assignment of the highest energy bands. Minimal basis set (STO-3G) calculations, although quantitatively less accurate, reproduce the qualitative relationships among these orbital energies. Both phosphirane and thiirane show a first band in the photoelectron

---

(1) (a) University of California, Santa Barbara; (b) California State University, Los Angeles; (c) University of California, San Francisco.

(2) (a) D. H. Aue, H. M. Webb, and M. T. Bowers, *J. Am. Chem. Soc*,., **97**, 4137 (1975); (b) R. I. Wagner, L. D. Freeman, H. Goldwhite, and D. G. Rowsell, *ibid*., **89**, 1102 (1967).

(3) (a) D. H. Aue, H. M. Webb, and M. T. Bowers, *J. Am. Chem. Soc*., **98**, 311 (1976); (b) D. H. Aue and M. T. Bowers in "Gas Phase Ion Chemistry", Vol. 2, M. T. Bowers, Ed., Academic Press, New York, 1979.

(4) W. R. Davidson, M. T. Bowers, T. Su, and D. H. Aue, *Int. J. Mass Spectrom. Ion Phys*., **24**, 83 (1977).

(5) W. Lathan, R. Ditchfield, M. D. Newton, and J. A. Pople, Quantum Chemistry Exchange Program No. 236.

(6) W. Hehre, R. F. Stewart, and J. A. Pople, *J. Chem. Phys*., **51**, 2657 (1969).

(7) R. Ditchfield, M. D. Newton, W. J. Hehre, and J. A. Pople, *J. Chem. Phys*., **54**, 724 (1971).

(8) H. Basch, M. B. Robin, N. A. Kuebler, C. Baker, and D. W. Turner, *J. Chem. Phys*., **51**, 52 (1969).

(9) A. D. Walsh, *Nature (London)*, **159**, 167, 712 (1947).

(10) C. A. Coulson and W. E. Moffit, *Philos. Mag*., **40**, 1 (1949).

(11) This work. Cf. spectra of alcohols: M. B. Robin and N. A. Kuebler, *J. Electron Spectrosc. Relat. Phenom*., **1**, 13 (1972).

0002-7863/80/1502-5151$01.00/0

Table I. Vertical Ionization Potentials and Orbital Energies of Three-Membered Heterocycles[a]

azirane			phosphirane			oxirane			thiirane		
orbital	exptl[a,b]	calcd[d]	orbital	exptl[b]	calcd[e]	orbital	exptl[b,c]	calcd[d]	orbital	exptl[b]	calcd[f]
a'(n)	9.83	10.50	a'(n)	9.75	9.88	b_1(n)	10.56	12.30	b_1(n)	9.03	9.36
a"(σ_a)	11.79	12.69	a"(σ_a)	10.21	10.20	a_1(σ_s)	11.85	12.30	b_2(σ_a)	11.37	11.51
a'(σ_s)	12.16	13.39	a'(σ_s)	11.78	12.33	b_2(σ_a)	13.73	14.69	a_1(σ_s)	11.93	11.71
a"($\pi^a{}_{CH_2}$)	13.45	14.64	a"($\pi^a{}_{CH_2}$)	13.10	14.18	a_2(π_{CH_2})	14.16	15.04	a_2(π_{CH_2})	13.51	14.91
a'(σ)	15.69	17.37	a'(σ)	14.75	15.83	a_1(n)	16.52	17.81	a_1(n)	15.33	16.43
a'($\pi^s{}_{CH_2}$)	17.19	19.14	a'($\pi^s{}_{CH_2}$)	16.0	17.76	b_1(π_{CH_2})	17.20	19.53	b_1(π_{CH_2})	16.58	18.5

[a] All values in eV. [b] This work. [c] Values agree with those in ref 8. These orbital symmetries have been relabeled with the b_1 and b_2 labels reversed from ref 8. Also our 4-31G calculations show similar energy ordering. [d] "Double-ζ" calculations from ref 8. [e] This work (4-31G calculations). Corresponding STO-3G calculations gave orbital energies of 7.92, 8.03, 10.68, 12.88, 14.19, and 16.29 eV in the same orbital energy order. [f] This work (STO-431G calculations). STO-3G calculations with 3d STOs from R. Bonaccorsi, E. Scrocco, and J. Tomasi, *J. Chem. Phys.*, 52, 5270 (1979), give comparable orbital energies and ordering.

Table II. Vertical Ionization Potentials and Orbital Energies of Me_2NH, Me_2PH, Me_2O, and Me_2S[a]

dimethylamine			dimethylphosphine			dimethyl ether			dimethyl sulfide		
orbital	exptl[b]	calcd[c]	orbital	exptl[d]	calcd[c]	orbital	exptl[e]	calcd[c]	orbital	exptl[e]	calcd[c]
a'(n)	8.93	9.71	a'(n)	9.10	9.12	b_1(n)	10.01	11.36	b_1(n)	8.68	9.03
a"(σ_{CN})	12.62	13.59	a"(σ_{CP})	11.8	12.36	a_1(n)	11.90	12.66	a_1(n)	11.35	11.30
a'(σ_s)	13.2	14.00	a'(σ_s)	12.1	12.62	b_2(σ_{CO})	13.55	14.42	b_2(σ_{CS})	12.75	13.29
a"($\pi^a{}_{CH_3}$)	13.8	14.75	a"($\pi^a{}_{CH_3}$)	13.65	15.04	a_2($\pi^a{}_{CH_3}$)	14.20	15.11	a_2($\pi^a{}_{CH_3}$)	14.25	15.39
a"(σ_{CN})	15.1	15.76	a"(σ_{CP})	14.15	15.14	b_2(σ_{CO})	16.4	17.03	b_2(π_{CS})	14.90	15.63
a'(π_{CH_3})	15.4	16.77	a'(σ)	15.0	15.95	a_1(σ_s)	16.4	17.63	a_1(σ_s)	15.5	16.44
a'(σ)	16.65	17.88	a'($\pi^s{}_{CH_3}$)	15.0	16.22	b_1($\pi^s{}_{CH_3}$)	16.4	18.00	b_1($\pi^s{}_{CH_3}$)	15.5	16.44

[a] All values in eV. [b] This work. See also ref 3a. [c] This work (4-31G calculations). [d] Reference 12. [e] This work. See also K. Watanabe, T. Nakayama, and J. Motil, *J. Quant. Spectrosc. Radiat. Transfer*, **2**, 369 (1962).

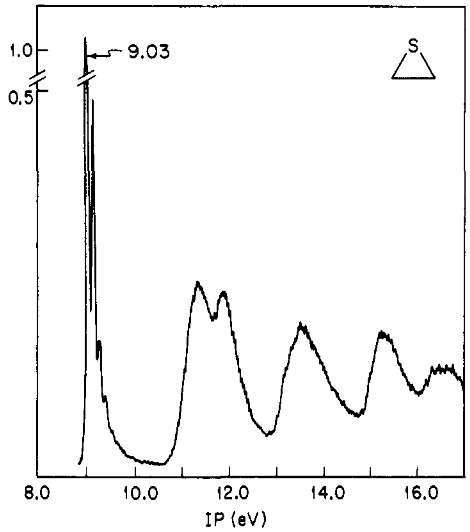

Figure 1. Photoelectron spectrum of thiirane at 25 °C.

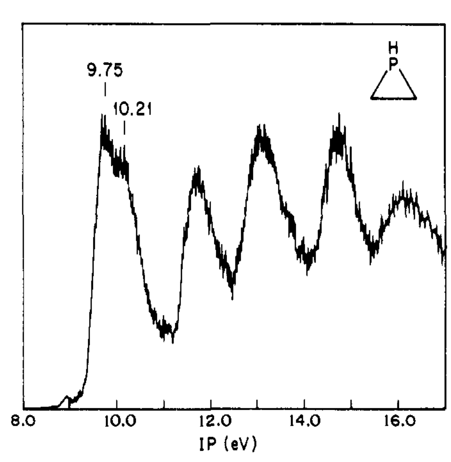

Figure 2. Photoelectron spectrum of phosphirane at 25 °C.

Table III. Comparisons of Experimental and STO-431G Calculated Proton Affinity and Ionization Potential Changes in N, P, O, and S Heterocycles on Ring Closure[a,b]

	azirane	phosphirane	oxirane	thiirane
ΔPA_{exptl}, kcal/mol	4.8 (2.7)[c]	22.3 (18.2)[c]	3.5 (0.8)[c]	4.9 (0.9)[c]
ΔPA_{calcd}[d]		21.9		
ΔPA_{calcd}(HXH), kcal/mol[d]	0.2	23.9	14.0	5.7
$\Delta\angle$RXR, deg[e]	3	16	7	4–5
$\Delta IP(n)_{exptl}$, eV	0.90	0.65	0.55	0.35
$\Delta IP(n)_{calcd}$, eV	0.79	0.76	0.94	0.33
$\Delta IP(n)(HXH)_{calcd}$, eV	0.62	0.41	0.35	0.11
$\Delta IP(n,a_1)_{exptl}$, eV			4.4	4.0
$\Delta IP(n,a_1)_{calcd}$, eV			5.15	5.13
$\Delta IP(n,a_1)(HXH)_{calcd}$, eV			1.74	0.05
$\Delta IP(\sigma_a)$, eV	−0.83	−1.6	0.18	−1.38
$\Delta IP(\sigma_a)_{calcd}$, eV	−0.90	−2.16	0.27	−1.78
$\Delta IP(\pi^a{}_{CH_2})$, eV	−0.3	−0.55	−0.04	−0.74
$\Delta IP(\pi^a{}_{CH_2})_{calcd}$, eV	−0.11	−0.86	−0.07	−0.48
$\Delta IP(\pi^s{}_{CH_2})$, eV	1.8	1.0	0.8	1.1
$\Delta IP(\pi^s{}_{CH_2})_{calcd}$, eV	2.27	1.54	1.53	2.1

[a] All energies in kcal/mol. [b] ΔPA and ΔIP refer to changes in proton affinities and ionization potentials between the three-membered heterocycles and corresponding dimethyl compounds and between HXH compounds of different bond angles (Table VII). [c] Corrected for polarizability changes on cyclization; see Table IV, footnote *m*. [d] From Table VII. [e] From Table VI.

spectrum that is assigned lone-pair character on the basis of these MO calculations and on the basis of the similarity of their vibrational Franck-Condon factors to the lone-pair bands of dialkylphosphines[12] and dialkyl sulfides.[13] The two Walsh-type orbitals for phosphirane and thiirane occur with the antisymmetric (σ_a) Walsh orbitals higher in energy than the symmetric (σ_s) Walsh orbitals. The photoelectron spectra of dimethylamine, dimethylphosphine,[12] dimethyl ether, and dimethyl sulfide have been measured for comparison and their orbital energies assigned in Table II and Scheme I on the basis of 4-31G level calculations.

The relative orbital energies for these heterocycles are shown in Scheme I. From this scheme the lone-pair orbital energies are

---

(12) M. F. Lappert, J. B. Pedley, B. T. Wilkins, O. Stelzer, and E. Unger, *J. Chem. Soc., Dalton Trans.*, 1207 (1975).

(13) This work. Cf. H. Bock and G. Wagner, *Angew. Chem., Int. Ed. Engl.*, **11**, 150 (1972).

Scheme I. Correlation Diagram for Experimental Orbital Energies of Three-Membered Heterocycles and Corresponding Dimethyl Analogues

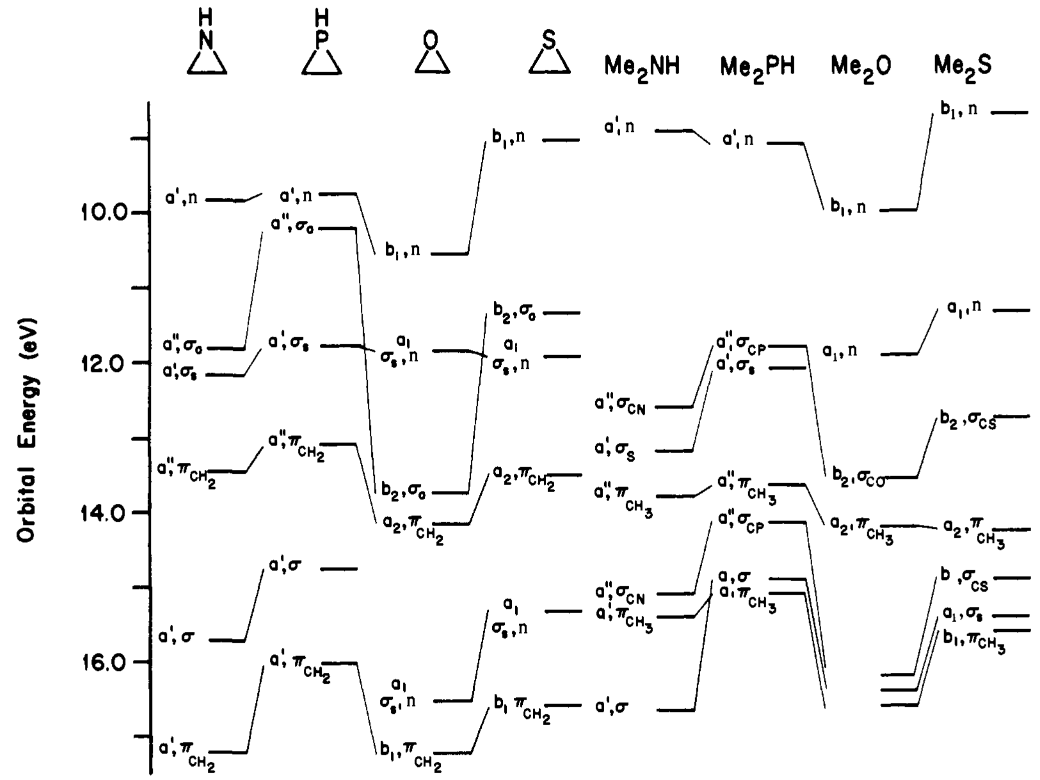

Table IV. Proton Affinities, Adiabatic and Vertical Ionization Potentials, and Hydrogen Affinities at 25 °C[a]

	GB[b]	PA	aIP[g]	aHA[k]	vIP	vHA[l]	ΔPA	ΔvIP
azirane	207.5[b]	215.7	213	115	226.7[h]	127.3	4.8	20.8
Me_2NH	212.3[b,d]	220.5	190	93	205.9[d]	111.3	(2.7)[m]	(15.2)[m]
phosphirane	186.6[c]	194.8	216	96	224.8	104.5	22.3	15.0
Me_2PH	208.9[e]	217.1[e]	195	97	209.8[i]	111.4	(18.2)[m]	(10.4)[m]
oxirane	182.3	189.6	240	115	243.5[j]	118.0	3.5	10.6
Me_2O	185.8	193.1	226	104	232.9[k]	110.9	(0.8)[m]	(4.0)[m]
thiirane	188.5	195.8	206	87	208.2	88.9	4.9	8.0
Me_2S	193.4[f]	200.7	197	84	200.2[k]	85.8	(0.9)[m]	(2.2)[m]

[a] All values in kcal/mol. [b] Gas-phase basicities are based on a recent GB scale based on GB(NH_3) = 196 and PA(NH_3) = 205 kcal/mol; ref 3b; R. Yamdagni and P. Kebarle, *J. Am. Chem. Soc.*, 98, 1320 (1976); J. F. Wolf, R. H. Staley, I. Koppel, M. Taagepera, R. T. McIver, J. L. Beauchamp, and R. W. Taft, *ibid.*, 99, 5417 (1977); however, see also F. A. Houle and J. L. Beauchamp, *ibid.*, 101, 4067 (1979). [c] A qualitative, nonequilibrium GB for phosphirane has been measured: Z. C. Profous, K. P. Wanczek, and H. Hartmann, *Z. Naturforsch. A*, 30, 1470 (1975); Abstracts 24th Conference on Mass Spectrometry and Allied Topics, San Diego, Calif., May 2976, No. Y12. [d] Reference 3. [e] R. H. Staley and J. L. Beauchamp, *J. Am. Chem. Soc.*, 96, 6252 (1974). [f] Adiabatic IPs are measured at the onset of the first band. [g] D. H. Aue, W. R. Davidson, W. D. Betowski, and M. T. Bowers, unpublished work; ref 3b. [h] The measurement from this work agrees with those of ref 8 and K. Yoshikawa, M. Hashimoto, and I. Morishima, *J. Am. Chem. Soc.*, 96, 289 (1974). We note a distinct eight-peak vibrational progression on the leading edge of the first bands, $\nu = 710\ cm^{-1}$. [i] Reference 12. [j] The measurement from this work agrees with those of footnote *g*. [k] The measurement from this work agrees with that of K. Watanabe, T. Nakayama, and J. Motil, *J. Quant. Spectrosc. Radiat. Transfer*, 2, 369 (1962). [l] Calculated using IP(H) = 315.1 kcal/mol: "JANAF Thermochemical Tables," *Natl. Stand. Ref. Data Ser., Natl. Bur. Stand.*, No. 37 (1971). [m] ΔPA and ΔvIP values in parentheses are corrected to account for the loss of one pair of electrons on ring closure of the dimethyl derivative to the heterocycle. The effect of the lost electron pair is taken to be one-third the effect on the PA and IP of adding the three electron pairs of a CH_2 group in going from CH_3X-H to CH_3X-CH_2-H. The PA and IP data are taken from ref 3ab, 12, footnote *e*, and J. F. Wolf, R. H. Staley, I. Koppel, M. Taagepera, R. T. McIver, J. L. Beauchamp, and R. W. Taft, *J. Am Chem. Soc.*, 98, 1320 (1976). The IP corrections (kcal/mol) are 16.9/3 = 5.6 (X = NH); 13.8/3 = 4.6 (X = PH); 19.8/3 = 6.6 (X = O); 17.5/3 = 5.8 (X = S). The PA corrections (kcal/mol) are 6.4/3 = 2.1 (X = NH); 12.3/3 = 4.1 (X = PH); 8.2/3 = 2.7 (X = O); 12.1/3 = 4.0 (X = S).

similar for azirane and phosphirane, while that of oxirane is lower and that of thiirane is higher. The relative ordering is identical with that of the corresponding dimethyl derivatives. The low orbital energies for oxirane and dimethyl ether reflect the high electronegativity of oxygen among other factors. For other comparable lower energy orbitals, the orbitals of the oxygen derivatives usually are at the lowest energies in Scheme I.

The differences in vertical ionization potentials (ΔvIP) between the lone-pair orbitals of oxirane and dimethyl ether and between thiirane and dimethyl sulfide are similar (Tables III and IV). Ring formation, in both cases, causes an 8–11 kcal/mol lowering in the lone-pair orbital energy. For azirane and phosphirane, a larger (15–21 kcal/mol) stabilization of the lone-pair orbitals occurs on ring closure. The comparison of the ionization potentials of these heterocycles with those of corresponding dimethyl derivatives is expected to result in approximate cancellation of the hyperconjugation and polarizability effects which play a large role in stabilizing radical cations resulting from ionization.[3] The differences in IP between the heterocycles and dimethyl derivatives could then be attributed to effects of the ring strain. In unstrained five- and six-membered rings (pyrrolidines and piperidines), however, similar comparisons of vIPs and PAs with dialkylamines reveal that the ring-closed molecules have higher vIPs and lower PAs by amounts which can be approximately correlated quantitatively with the loss of one electron pair on ring closure.[3] In light of these facts, we have attempted to refine the comparisons of the three-membered heterocycles by assuming that one-third of the stabilizing effect of the six extra electrons of the last added methyl group in $CH_3X^{+\cdot}$–CH_2–H vs. $CH_3X^{+\cdot}$–H is lost on ring closure to $\overline{CH_2X^{+\cdot}CH_2}$. Such corrections have been applied to the ΔvIP and ΔPA values in Tables III and IV and are explained in the footnote to Table IV. The corrected ΔvIP and ΔPA data are shown in parentheses in these tables. From detailed consideration of the geometric locations of the electrons involved and from consideration of the attenuation of the effects of successive added electron pairs,[3a] we expect that these corrections to ΔvIP and ΔPA are overestimates of the effect of the electron pair lost on cyclization. The corrected ΔvIP and ΔPA values then appear to be lower limits to the ring-strain effect, and the "true" ring-strain effect probably lies between the corrected and uncorrected values.

The stabilization of the lone-pair orbital in azirane and phosphirane can, in part, be attributed to an increased fraction of s character in the lone pair on ring closure. The b_1 lone-pair orbitals in ethers and sulfides, however, are both pure p orbitals, so no change in s character is possible for these orbitals on cyclization.[14] Some other factor, then, must account for the energy lowering of the b_1 orbitals in oxirane and thiirane. One possible explanation might come from Walsh's rule arguments[15] based on a predicted increase in the bonding interaction between the p components of the b_1 orbitals on the carbons as the angle between the carbons decreases. Calculations on water and hydrogen sulfide at constrained bond angles (Tables III and VII), however, reproduce the stabilization effects (ΔIP(n), Table III) on the b_1 orbitals in oxirane and thiirane, even though there can be no p component in the hydrogens to produce the Walsh's rule effect above. Thus, another explanation is required. Examination of the charge densities on X and H in H_2O and H_2S (Table VII) shows that electron density in the σ bonds shifts toward the hydrogens as the HXH bond angle decreases because of increased repulsion of the bonding electrons close to X. This shift in electron density makes X more positive when the HXH angle is decreased and results in a stabilization of the b_1 p orbital on X. This effect appears to provide an adequate explanation of the b_1 lone-pair ionization potentials in oxirane and thiirane relative to dimethyl ether and dimethyl sulfide, respectively.

For azirane and phosphirane, the effects of ring closure on the lone-pair ionization potentials (ΔvIP) are 20.8 and 15.4 kcal/mol, respectively. These effects could, in part, be the result of factors such as those operating in oxirane and thiirane, but the remainder of this large ionization-potential change is attributable to an increase in s character in the N and P lone pairs on ring closure. Indeed, the calculated s characters for the lone pairs in constrained PH_3 and NH_3 show these hybridization effects (Table VII and III). The calculations for N, P, O, and S hydrides nicely reproduce the relative magnitudes of ΔIP(n) through the series (Table III). The calculated orbital energies for the actual heterocycles and dimethyl compounds (Tables I–III) better reproduce the absolute values of ΔIP(n) except for the ΔIP(n) for oxirane, which shows a rather high $\Delta IP(n)_{calcd}$.

The second lone-pair orbitals (a_1, n) in oxirane and thiirane strongly mix with the a_1, σ_s orbitals making an analysis of the energies of these orbitals complicated. The corresponding orbitals in dimethyl ether and sulfide do not mix nearly as strongly because of a wider energy gap and spatial separation.[16] The lower energy a_1 orbitals have predominant lone-pair character in oxirane and thiirane. Their energies are considerably lower (Table III) than expected simply from the increased s character in their orbitals (Table VII) relative to the a_1 lone-pair orbitals in dimethyl ether and sulfide. A large part of this enegy lowering must result from the strong interaction of the a_1, n and a_1, σ_s orbitals. If, for comparison with the a_1, n orbitals in dimethyl ether and sulfide, an upper limit on the energies of the "pure" a_1 lone-pair orbitals is taken as the approximate average of the higher and lower energy a_1 orbitals in oxirane and thiirane, then more than a 2-eV lowering of the lone-pair energy in these heterocycles can be attributed to the increase in s character in these orbitals (Table VII). In oxirane and thiirane, the higher energy a_1 orbitals have a large amount of σ_s character and are at about the same energy as the a′, σ_s orbitals in azirane and phosphirane. These a_1 orbitals may be at higher energy than expected relative to the a′, σ_s orbitals in azirane and phosphirane. They seem to interact a little more strongly with the other a_1 orbitals than do the a′, σ_s and a′, σ orbitals in azirane and phosphirane.[16]

The antisymmetric Walsh orbitals (σ_a) in the heterocycles do not interact with other orbitals and are nicely localized in the C–X bonds. They vary widely with the nature of the heteroatom X in a manner that is similar to the energy changes of the corresponding antisymmetric σ_{C-X} in the dimethyl derivatives (Scheme I). A detailed analysis of the differences in IP, ΔIP(σ_a), in Table III on ring closure reveals some interesting effects. The energies of the σ_a orbitals in all cases except oxirane are raised by ring closure, but the increase in energy is considerably larger for phosphirane and thiirane than for azirane. These changes are well reproduced in the calculated ionization potentials (Table III), even for oxirane. The increase in energy of σ_a orbital on ring closure doubtless results from aggravation of the antibonding interaction in σ_a as the RXR bond angle decreases. The change in this bond angle is largest for thiirane and phosphirane and occurs between smaller angles where the antibonding interactions are strongest. This provides an explanation for the large effects seen in phosphirane and thiirane. The reversal in ΔIP(σ_a) in oxirane, however, is not readily explicable, though its change in bond angle is slightly smaller than for azirane.

The symmetric and antisymmetric π-type orbitals localized on the CH_2 and CH_3 groups maintain their character throughout the series of compounds with little or no mixing with other orbitals. The changes in the energy of the antisymmetric orbital, $\pi^a{}_{CH_2}$, on ring closure closely parallel to the calculated changes in Table III and show the same pattern as observed above for the antisymmetric Walsh orbitals, σ_a. Even the negligible effect in $\pi^a{}_{CH_2}$ for oxirane compares well with the slight reversal observed for the σ_a orbital. The increased orbital energies on ring closure, again, appear to result from increased antibonding interaction at smaller angles. As expected, the symmetric $\pi^s{}_{CH_2}$ orbitals show just the opposite effect. Their energies are significantly lowered as the bonding interactions in these $\pi^s{}_{CH_2}$ orbitals increase on cyclization.

The reasonable variation in these orbital energies in comparison with calculated energies and qualitative theories helps to support the assignments of these photoelectron spectra.

Proton Affinities. The proton affinities of the heterocycles studied are compared with those of model open-chain dimethyl analogues of similar polarizability in Table II. The differences in PA (ΔPA) in Table II show similar 3–5 kcal/mol lowerings in the PAs for azirane, oxirane, and thiirane relative to their ring-opened models, but phosphirane shows a much larger 23.2 kcal/mol effect in the same direction. We have previously explained these effects in azirane and oxirane as lone-pair hybridization effects, wherein the increased s character in the lone-pair orbitals of the heterocycles makes protonation less favorable than in open-chain analogues.[1] While this explanation seems adequate to explain the PA effects in azirane, oxirane, and even thiirane, it does not appear capable of explaining the anomalously low PA of phosphirane. A consideration of the changes in bond angle strain effects in this series of heterocycles provides an explanation for the phosphirane case.

The strain energy of a molecule or ion is expected to be related to the difference between its bond angles and those in an analogous unconstrained molecule or ion.[17] For the heteroatoms in question, a set of largely experimental bond angles is available for the atomic hydrides and their ions (Table VI). The bond angles in azirane and oxirane are constrained to 69 and 73°, respectively (Table

---

(14) D. A. Sweigart, *J. Chem. Educ.*, **50**, 232 (1973).

(15) A. D. Walsh, *J. Chem. Soc.*, 2260 (1953).

(16) Orbital drawings for azirane, oxirane, and dimethyl ether may be found in W. L. Jorgensen and L. Salem, "The Organic Chemist's Book of Orbitals", Academic Press, New York, 1973.

(17) P. v. R. Schleyer, J. E. Williams, and K. R. Blanchard, *J. Am. Chem. Soc.*, **92**, 2377 (1970); H. C. Brown, R. C. Fletcher, and R. B. Johannsen, *ibid.*, **73**, 212 (1951).

Table V. Experimental Free Energies for Proton Transfer in the Equilibria $AH^+ + B \rightleftarrows BH^+ + A$[a]

A	B	ΔG°[b]	GB(B)[c]
azirane	$EtNH_2$	−1.15[d]	208.7
azirane	$CH_2{=}CHCH_2NH_2$	−0.55[d]	208.1
azirane	3-chloropyridine	−0.2[d]	207.9
azirane	3-fluoropyridine	+0.5[d]	207.0
azirane	$MeNHNH_2$	+1.47[d]	206.3
azirane	$CC_3H_5NH_2$	−0.9 ± 0.1[d,e]	204.5
oxirane	MeC≡N	−0.6, −0.8[d]	183.1
oxirane	EtOH	−0.3	182.5
oxirane	$(CF_3)_3CNH_2$	−1.2,[d] −1.4	183.1
thiirane	MeOAc	−1.8 ± 0.2	190.5
thiirane	$CH_3CH{=}C(CH_3)_2$	−1.1 ± 0.2	188.5
thiirane	$CH_2{=}C(CH_3)_2$	+0.2 ± 0.2[e]	188.3
thiirane	HCOO-*n*-Bu	+0.5 ± 0.1[e]	188.0
phosphirane[f]	HCOO-*n*-Pr	−0.7 ± 0.2	187.4
phosphirane	Me_2O	+0.5 ± 0.1	185.8
phosphirane	dioxane	−0.5 ± 0.1	187.2

[a] All values in kcal/mol. [b] Error limits indicate reproducibility of multiple runs at different pressure ratios of A and B. Measured in a trapped ion cell unless otherwise indicated. [c] Values derived from ref 3a,b. [d] Measured in a drift cell at high pressures ($>10^{-4}$ Torr). [e] Approximate rates of proton transfer and ion loss from ejection measurements in trapped ion cell experiments indicate that equilibrium is achievable; see ref 4. [f] Additional double-resonance experiments for phosphirane with Et_2O, MeOAc, oxetane, and Me_2O indicate that the GB of phosphirane is between 185.8 and 189.6 kcal/mol.

Table VI. Experimental Geometries of N, P, O, and S Compounds

	exptl ∠RXR,[a] deg	ΔRXR, deg
H_3N	106.7	
H_4N^+	109.5	3
Me_2NH	111	
H_3P	93.5	
H_4P^+	109.5	16
Me_2PH	99.4	
H_2O	104.5	
H_3O^+	(110)[b]	5.5
Me_2O	111	
H_2S	92.5	
H_3S^+	(97.5)[c,d]	5
Me_2S	100	

[a] See *Chem. Soc., Spec. Publ.*, No. **11** (1958); No. 18 (1965). [b] This is a near Hartree–Fock calculation by C. F. Bender and P. A. Kollman, *Chem. Phys. Lett.*, **21**, 271 (1973). [c] Our calculations here on H_2S find $\theta(HSH) = 96^\circ$ and on H_3S^+ find $\theta(HSH) = 101^\circ$; thus, we think that a $\Delta\theta \approx 5^\circ$ is a reasonable estimate. [d] Recent calculations give 94.5°; D. A. Dixon and D. S. Mangnick, *J. Chem. Phys.*, 71, 2860 (1979).

VII). These differ from the larger bond angles in NH_3 and H_2O causing considerable strain in those molecules. The bond angles in NH_4^+ and H_3O^+ are only 3 and 5° larger, respectively, than in NH_3 and H_2O, so we expect the protonated azirane and oxirane are strained only slightly more than the neutral heterocycles. Similarly, the increase in angle from H_2S to H_3S^+ is only about 5°, but the bond angle in PH_3 increases by 16° on protonation to PH_4^+. This large change in bond angle on protonation, therefore, could explain, in large part, the low proton affinity of phosphirane.

We carried out a series of ab initio calculations for some of these molecules and ions in order to better define the effects postulated to explain their relative stabilities. The percent s character was determined for the series of hydrides in Table VII at their unconstrained optimum geometries and at bond angles corresponding to those in the three-membered heterocycles. The increase in percent s character in NH_3 is 9% and that in PH_3 is 18% on constraint, perhaps suggesting a larger change in proton affinity in the phosphorus case, although the calculated change in s character from dimethylphosphine to phosphirane is only 6%. The s character increases in the a_1 lone pairs of H_2S and H_2O are 19 and 25%, respectively. Since these a_1 orbitals and the b_1 orbital (0% s character) are mixed more or less equally after protonation in the lone-pair and bond-pair orbitals of the ion, it seems appropriate to divide these increases in half for comparison with NH_3 and PH_3. This gives increases in percent s character of ca. 10% for NH_3, H_2S, and H_2O.

These calculations and the changes noted in the ionization potentials suggest that there are indeed significant changes in lone-pair s character in these three-membered heterocycles which could be responsible for a lowering of their proton affinities. The increase in angle strain on protonation also appears to be a significant factor, however, and probably the dominant factor for phosphirane.

Because we wished to investigate the effect of strain on proton affinities in a general way, we first focused on model calculations of NH_3, H_2O, H_2S, and PH_3. We evaluated the proton affinities for these compounds and compared them with the proton affinities calculated when we forced one of the H–X–H (X = P or S) angles to be constrained to the observed angle in the three-membered ring (Table VII). We kept all r(S–H) = 1.33, r(P–H) = 1,42, r(N–H) = 1.01, and r(O–H) = 0.96 Å and optimized the remaining angles for both protonated and unprotonated compounds. To validate this approach, we calculated the proton affinity of phosphirane directly and compared it to that of $(CH_3)_2PH$. The 4-31G calculation on protonated phosphirane did not converge, so we report the STO-3G calculations for that case. A set of reference STO-3G calculations on the proton affinities of the strained and unstrained phosphine showed that the basis set reproduces the qualitative relationships between angle and proton affinity.

Our calculations on H_2S and PH_3 are in agreement with experiment. In Table II it is seen that the proton affinity of a strained PH_3 is 23.2 kcal/mol less than that of the "normal" molecule. The proton affinity of a comparably deformed H_2S is reduced by only 5.7 kcal/mol. The STO-3G calculated proton affinity of phosphirane, relative to the parent dimethylphosphine, is reduced by 21.9 kcal/mol, an amount remarkably close to that calculated in the PH_3 model. These calculations thus lend strong support to our proposal that proton affinities of cyclic compounds are dependent upon the relative deformations of the neutral and the protonated species.

The calculations on unstrained and strained models for the protonation of H_2O and NH_3 are not consistently successful in reproducing the difference in proton affinities between the cyclic ring compounds and the unstrained dimethyl compounds. A plausible explanation for this is the inadequacy of a 4-31G basis set in reproducing experimental HXH angles in the second-row hydrides (in contrast to its relative accuracy for the third row). For unstrained and strained NH_3, surprisingly, the energy difference is calculated to be near zero. A 4-31G basis set predicts θ (HNH) in NH_3 to be 116° (rather than 107°). Thus, in the 4-31G model strained hydride, there is more "strain" in the neutral molecule than the protonated, where the unstrained angle is 109.5°. The 4-31G predictions for θ (HOH) are 112° for H_2O and 120° for H_3O^+. Thus, in this case, one has more strain in the protonated than the neutral hydride and the 14 kcal/mol proton affinity difference between the unstrained and strained H_2O is consistent with this. However, the model calculations do overestimate the difference in proton affinity between $(CH_2)_2O$ and $(CH_3)_2O$. We expect that a hydride model is less adequate for the second-row hydrides than the third, because, in this model, the nonbonded HXH interactions are larger, especially in the protonated species, because of the larger partial charge on the hydrogens. The fact that the difference in proton affinities in model NH_3 is not overestimated is probably due to the incorrect representation of the HNH angle in NH_3 compared to NH_4^+.

In order to gain further insight into the way in which changes in bond angles effect energies of protonation, we did a Morokuma component analysis[18] on the proton affinities of PH_3 and NH_3

---

(18) S. Iwata and K. Morokuma, *J. Am. Chem. Soc.*, **95**, 7563 (1973); P. Kollman and S. Rothenberg, *ibid.*, **99**, 1333 (1977).

Table VII. Properties of O, S, N, and P Compounds from STO-431 G Calculations

	RXR angle, deg	s coefficient[a]	p coefficient[a]	% s character[a]	charge on X[b]	lone pair IPs, eV	PA calcd, kcal/mol	ΔPA calcd,[b] kcal/mol	dipole moment, D	
									calcd	exptl[n]
H_2O	112[c]	0.321	0.418	43	−0.78	13.60 (b_1), 15.17 (a_1)	183.1			
	73.2[d,e]	0.649	0.306	68	−0.70	13.95 (b_1), 16.91 (a_1)	169.1	14.0		
NH_3	116[c]	0.259	0.520	33	−0.90	11.26	222.8			
	69.4[f,g]	0.342	0.478	42	−0.83	11.88	222.6	0.2		
H_2S	96[h]	0.466	0.405	54	−0.18	10.41 (b_1), 13.11 (a_1)	160.5			
	48.4[i,j]	0.622	0.229	73	−0.14	10.52 (b_1), 13.16 (a_1)	154.8	5.7		
PH_3	96[h]	0.550	0.592	48	+0.06	10.36	187.2			
	47.4[k,l]	0.756	0.396	66	+0.05	10.77	163.3	23.9		
azirane	69.4[f]	0.207	0.461	31	−0.64	10.50			2.42	1.90
Me_2NH	109[p]	0.157	0.525	23	−0.71	9.71			1.56	1.03
phosphirane	47.4[k]	0.505	0.534	49	+0.33	9.88	239.5[m]	21.9	1.13	1.12
Me_2PH	99.4[p]	0.477	0.624	43	+0.39	9.12	261.4[m]		1.14	1.23
oxirane	73.2[d]	0.095	0.335	22	−0.61	12.30 (b_1), 12.30 (a_1)			2.89	1.89
		(0.191)[o]	(0.212)[o]	(47)[o]						
Me_2O	111[p]	0.175	0.407	30	−0.70	11.36 (b_1), 12.66 (a_1)			2.05	1.30
		(0.064)[o]	(0.202)[o]	(24)[o]						
thiirane	96[i]	0.310	0.319	49	+0.10	9.35 (b_1), 11.69 (a_1)			2.19	1.85
		(0.353)[o]	(0.068)[o]	(84)[o]						
Me_2S	100[p]	0.403	0.403	50	+0.14	9.03 (b_1), 11.30 (a_1)			1.83	1.50
		(0.019)[o]	(0.108)[o]	(15)[o]						

[a] From the coefficients of outer s and p orbital in lone pair. Data are for the a_1 lone pairs. [b] Mulliken partial charge on lone-pair atom in H_nX^+. [c] 431G optimized structure; see W. Lathan, W. Hehre, L. Curtiss, and J. A. Pople, *J. Am. Chem. Soc.*, 93, 6377 (1971). [d] Experimental COC angle in oxirane. See footnote *a* Table VI. [e] Optimum angle between H and bisector of $H_2O = 50°$ for H_3O^+ with two hydrogens constrained to $\theta = 73.2°$. [f] Experimental CNC angle in azirane. See footnote *a*, Table VI. [g] Optimum HNH angle for the two nonconstrained hydrogens (C_{2v} symmetry) = 116°. [h] Optimized HXH angle. [i] Experimental angle in thiirane. See footnote *a*, Table VI. [j] Optimum angle between H and bisector of H_2S is 48°. [k] Experimental angle in phosphirane. See footnote *n*. [l] Optimum HPH angle for the two unconstrained hydrogens = 130°. [m] STO-3G calculations. [n] From "Selected Values of Electric Dipole Moments for Molecules in the Gas Phase", *Natl. Stand. Ref. Data Ser., Natl. Bur. Stand.*, No. 10 (1967); M. T. Bowers, R. A. Beaudet, H. W. Goldwhite, and R. Tang, *J. Am. Chem. Soc.*, 91, 17 (1969). [o] Values from the lower energy a_1 orbitals. The lower energy a_1 orbital in oxirane has large lone-pair character and a large s character. The changes in the two a_1 orbitals in oxirane and Me_2O indicate an overall increase in s character in oxirane. [p] Experimental angles from footnote *a*, Table VI.

at a number of different HXH angles. In this analysis the total interaction energy between the moleuclar fragments is partitioned into the separate effects of electrostatic (nuclear and electronic charge interaction of the unperturbed fragments), polarization (intramolecular electronic rearrangement), and charge transfer (electronic rearrangement between the two fragments). The results of these calculations are in Table VIII. In phosphine the terms which measure the effect of charge redistribution upon protonation (polarization and charge transfer) nearly cancel one another. It is the charge redistribution in the neutral parent, as the angle is changed, which is principally responsible for the change in proton affinity. Narrowing the H–P–H angle from 109.5 to 60° drastically lowers the dipole moment of the molecule, reflecting a reduced negative charge and reduced p character in the lone pair in the vicinity of phosphorus. It is, of course, the interaction of this negative charge with the electropositive proton which is responsible for the negative term in the electrostatic energy. Consequently, as the angle is narrowed, the electrostatic energy rises from a negative value at the tetrahedral geometry to a positive, repulsive value at 60°.

In the case of ammonia, the dipole moment increases with decreasing angle, which is as one might expect from bond-moment additivity; this effect on dipole moment is not overwhelmed by the decrease in lone-pair moment, as found in PH_3. Despite the relative dipole moments, the electrostatic energy is smaller in magnitude at the smaller angle, reflecting the significantly smaller (Table VII) p character in the lone pair. In addition, this decrease in p character is reflected in the smaller magnitude charge transfer energy at the smaller angle because of less efficient overlap of the lone pair with the hydrogen 1s orbital.

The reason that the polarization energy is more favorable on protonation at smaller angles in phosphine, but remains unchanged at smaller angles in ammonia, may be that the energy gaps between the bonding and antibonding orbitals in ammonia and phosphine change differently with changing angle. The energy gap between the "e" symmetry bonding and antibonding X–H orbitals gets smaller more rapidly with decreasing angle for phosphine than for ammonia. Thus the increased mixing of these orbitals (polarization) at smaller angles is greater in the presence of the proton field in phosphine than in ammonia.

Table VIII. Component Analysis. Proton Affinity as a Function of Bond Angle in Phosphine and Ammonia[a]

	HXH bond angle		
	60°	90°	109.5°
Ammonia			
total energy (PA_{calcd}), kcal/mol		−169.2	−212.9
electrostatic energy, kcal/mol		−91.7	−110.1
polarization energy, kcal/mol		−23.1	−23.4
charge-transfer energy, kcal/mol		−54.4	−79.4
dipole moment of NH_3, D		2.96	2.60
phosphine			
total energy (PA_{calcd}), kcal/mol	−129.2	−168.9	−198.4
electrostatic energy, kcal/mol	+18.1	−21.9	−49.6
polarization energy, kcal/mol	−54.6	−32.3	−18.8
charge-transfer energy, kcal/mol	−92.7	−114.7	−130.0
dipole moment of PH_3, D	0.43	0.96	1.46

[a] Energies and dipole moments from 4-31G calculations. [b] Refers to HPH angle in the neutral molecule. The added proton is located along the molecular axis, leaving the other angles unchanged. Unlike the calculations in Table VII, all three HXH angles are constrained. $R(NH) = 1.16$ and $R(PH) = 1.60$ Å.

Conclusions

The effect of ring strain on the electronic structures for azirane, phosphirane, oxirane, and thiirane can be understood from a comparison of their photoelectron spectra with those of dimethyl analogues with the aid of ab initio STO-431G molecular orbital calculations. Increased s character in the lone-pair orbitals affects their ionization potentials from this analysis and it seems to affect the proton affinities of these molecules as well. From the proton-affinity data and from a Morokuma analysis of the important electrostatic and charge-transfer terms of these protonation energies in model calculations for constrained ammonia and phosphine, we note that increased s character in the lone pairs causes a decrease in the proton affinities. Increased s character decreases the lone-pair density in the region of the added proton, making the electrostatic energy term less favorable. The less favorable overlap between the lone-pair s character also makes the electrostatic energy less favorable. In the case of phosphirane, an additional internal bond angle strain (I-strain) increase in the conjugate acid causes the proton affinity to be unusually low.

Acknowledgments. We thank the National Science Foundation for support of this work.

Analysis of the Rotational Strength by Means of Configuration Analysis Based on the Localized Molecular Orbitals

Kazuo Akagi, Tokio Yamabe, Hiroshi Kato, Akira Imamura, and Kenichi Fukui*

Contribution from the Department of Hydrocarbon Chemistry, Faculty of Engineering, Kyoto University, Kyoto, Japan, the College of General Education, Nagoya University, Chikusa-ku, Nagoya, Japan, and the Shiga University of Medical Science, Seta, Ohtu, Japan.

Received January 21, 1980

Abstract: The n–π^* and π–π^* rotational strengths of the optically active L-5-methylpyrrolid-2-one molecule have been analyzed in detail by means of configuration analysis based on the LMO's presented here. This procedure has enabled us to evaluate simultaneously the contributions of the chromophore, substituent, and the rest of the molecule to the rotational strength of interest. The origin and effective path generating the rotational strength and their mechanisms have also been elucidated from the aspect of the intramolecular interactions between three or four molecular fragments in terms of the electronic configurations such as local and charge-transfer excitations.

I. Introduction

The rotational strengths in circular dichroism (CD) or optical rotatory dispersion (ORD) spectra have played central roles in the studies of optical activity, because of their outstanding sensitivities to the conformations and evironments.[1] The difficulties and/or ambiguities encountered in the interpretation of the rotational strengths, which have arisen from the structural complexies of molecules, have often let the investigators employ cyclic molecular systems having the restricted conformational freedom.[2] Especially, small cyclic molecules containing the peptide (amide)[3–6] and carbonyl chromophores[7] have become the focus of attention owing to their great importance in biochemistry as well as in organic chemistry. The considerable efforts to correlate the rotational strengths with the molecular structures have provided the empirical symmetry rules such as octant, quadrant, and sector rules, which are useful for defining the specific stereochemical features.[1,8,9] The approaches based on these symmetry rules, where the rotational strengths are interpreted with respect to the interaction between the chromophore and extrachromophoric moieties of a molecule, have presented the important concept of the intramolecular interaction in the chiroptical molecules,[10] by which the theoretical perturbation methods discussed later have been facilitated and developed. However, such approaches have been found to be insufficient for the explicit factorizations of the rotational strengths in terms of molecular fragments and also for the quantitative discussion, since the symmetry rules mentioned above not only permit considerable exceptions in determing the signs of the rotational strengths but also provide no features of electronic structure for interpreting the rotational strengths associated with the electronic transitions.[11]

In fact, there remain urgent problems to be solved concerning optical activity at the present stage, one of which is to clarify the origin of the optical activity determining the signs and magnitudes of the rotational strengths (e.g., inherent ring chirality and/or substituent asymmetrically linked with the chiral center).[3,5,12–14] Another is the verification of the mechanism and favorable path through which the electronic transitions of the locally symmetric chromophores are affected by the dissymmetric environment to yield the rotational strengths.[10] It is clear that these problems, that are also the subjects of our interest, are closely related to the intramolecular interaction. It follows therefore that the settlement of these problems depends upon the detailed analysis of the rotational strengths in terms of the intramolecular interaction derived from reliable theoretical calculations.

In the theoretical calculations of the rotational strengths, there have been two approaches such as perturbation methods[15–20] and

---

* To whom correspondence should be addressed at Kyoto University.

(1) (a) C. Djerassi, "Optical Rotatory Dispersion", McGraw-Hill, New York, 1960; (b) G. Snatzke, "Optical Rotatory Dispersion and Circular Dichroism in Organic Chemistry", Heyden, London, 1967.

(2) For instance, J. A. Schellman and E. B. Nielsen, "Conformation of Biopolymers", G. N. Ramachdran, Ed., Academic Press, New York, 1967.

(3) D. W. Urry, *Ann. Rev. Phys. Chem.*, **19**, 477 (1968).

(4) N. J. Greenfield and G. D. Fasman, *J. Am. Chem. Soc.*, **92**, 177 (1970).

(5) J. A. Schellman and S. Lifson, *Biopolymers*, **12**, 315 (1973).

(6) O. Červinka, L. Hub, F. Snatzke, and G. Snatzke, *Collect. Czech. Chem. Commun.*, **38**, 897 (1973).

(7) (a) J. P. Jennings, W. Klyne, and P. M. Scope, *J. Chem. Soc.*, 7211, 7299 (1965); (b) J. Listowski, G. Avigad, and S. England, *J. Org. Chem.*, **35**, 1080 (1970); (c) M. Keller and G. Snatzke, *Tetrahedron*, **29**, 4013 (1973); (d) T. D. Bouman and D. A. Lighter, *J. Am. Chem. Soc.*, **98**, 3145 (1976).

(8) W. Moffit, R. B. Woodward, A. Moscowitz, W. Klyne, and C. Djerassi, *J. Am. Chem. Soc.*, **83**, 4013 (1961).

(9) (a) J. A. Schellman and P. Oriel, *J. Chem. Phys.*, **37**, 2144 (1962); (b) J. A. Schellman and E. B. Nielsen, *ibid.*, **71**, 3914 (1967).

(10) (a) D. J. Caldwell and H. Eyring, "The Theory of Optical Activity", Wiley, New York, 1971; (b) A. Imamura and K. Hirao, *Tetrahedron*, **35**, 2243 (1979), see also the references therein.

(11) (a) W. Klyne, *Tetrahedron*, **13**, 29 (1961); (b) C. Ouannes and J. Jacques, *Bull. Soc. Chim. Fr.*, 3611 (1965); (c) D. N. Kirk and W. Klyne, *J. Chem. Soc., Perkin Trans. 1*, 1076 (1974).

(12) (a) H. Wolf, *Tetrahedron Lett.*, 1075 (1965): (b) M Goodman, C. Toniolo, and J. Falcetta, *J. Am. Chem. Soc.*, **91** 1816 (1969); (c) A. F. Beecham, *Tetrahedron Lett.*, 4897 (1969); (d) T. Konno, H. Meguro, and K. Tuzimura, *Tetrahedon Lett.*, 1305, 1309 (1975).

(13) (a) F. S. Richardson, D. D. Shillady, and J. E. Bloor, *J. Phys. Chem.*, **72**, 2466 (1971); (b) F. S. Richardson and R. W. Strickland, *Tetrahedron*, **31**, 2309 (1975).

(14) F. S. Richardson, R. Strickland, and D. D. Shillady, *J. Phys. Chem.*, **77**, 248 (1973).

0002-7863/80/1502-5157$01.00/0